Highlights of Spanish Astrophysics XI, Proceedings of the XV Scientific Meeting of the Spanish Astronomical Society held on September 4–9, 2022, in La Laguna, Spain. M. Manteiga, L. Bellot, P. Benavidez, A. de Lorenzo-Cáceres, M. A. Fuente, M. J. Martínez, M. Vázquez- Acosta, C. Dafonte (eds.), 2023

The separated star formation main sequence of bulges and discs. New clues for the galaxy mass assembly.

Méndez-Abreu, J[1,2], de Lorenzo-Cáceres, A.[1,2], and Sanchez, S. F.[3]

[1] Departamento de Astrofísica, Universidad de La Laguna, 38205, La Laguna, Tenerife, Spain
[2] Instituto de Astrofísica de Canarias, 38200, La Laguna, Tenerife, Spain
[3] Instituto de Astronomía, Universidad Nacional Autónoma de México, A.P. 70-264, 04510 México, D.F., México

Abstract

Disc galaxies are complex systems shaped by different stellar structures such as bulges, discs, and bars. Every galaxy structure keeps a unique memory of their past evolution, thus, understanding the mass assembly of disc galaxies can only be achieved by analysing separately all these independent footprints of past evolution. In this work, we have analysed the separated star formation main sequence (SFMS) of bulges and discs in the CALIFA sample. To this aim, we use the C2D algorithm to separate the spectra of bulges and discs using the information provided by the CALIFA integral field survey. We find that the star formation in galaxies mainly occurs in the disc component and not in bulges. Remarkably, once we only account for the disc mass, even the discs of early-type galaxies are compatible with the SFMS defined by star forming galaxies at z $\sim$ 0. Moreover, we find a strong mass depedence in the SFMS. For the bulges, only the low-mass bulges in late-type spirals ($\log M_{\star,\mathrm{b}}/M_{\odot} < 9$) are compatible with the SFMS of z $\sim$ 0 star-forming galaxies. The fraction of discs compatible with the SFMS is also a function of the disc (or total) stellar mass. Our results remark the importance of separating the spectral properties of different galaxy structures to provide a whole picture of the galaxy mass assembly throughout cosmic time.

1 Introduction

A powerful tool to study the evolution of the star formation rate (SFR) in galaxies is provided by scaling relations such as the star formation main sequence (hereafter, SFMS), a tight relation between a galaxy's SFR and its total stellar mass ($M_{\star}$; [1]). This relationship exists out to high redshifts, increasing its normalization to higher values at earlier epochs such that SFRs at a fixed stellar mass are higher by a factor of ~ 20 at $z \sim 2$ [5, 26]. The position of the

galaxies with respect to the SFMS, at any given epoch, gives us information about whether the SFR is enhanced or suppressed relative to the mean for their stellar mass. Despite the large amount of literature in the topic, most of the works on the properties of the SFMS have been limited to studies of star-forming galaxies. Nevertheless, it is known that ETGs remain well below the SFMS [23], with various processes invoked as responsible for the differences in SFR with respect to star forming galaxies. These include: i) internal structure (such as bars and bulges; [31]), cold gas fraction [25], interaction with other galaxies [30] and the presence of an AGN [10, 27].

Observationally, it has become increasingly clear that a general scenario to understand the trigger and shut-down of star-formation in galaxies must include a description on how this happens for their different stellar structures, in particular for their main components: bulges and discs. The difficulties inherent to identify, and separate, these structures have hindered most of our advance in this topic to photometry-based studies. They generally use standard photometric decomposition techniques applied to broad-band galaxy images [22, 21, 8, 6]. On the other hand, even after the revolution introduced by integral-field spectrographs, spectroscopic studies have been mostly limited to radial analysis of galaxies [12], or in the best cases to define regions where the light of each component (bulge and disc) dominates over the others using segmentation maps [9, 3, 7]. Fortunately, the necessity to understand the stellar population properties and mass growth of galactic structures have led to some methodological advances: i) spectro-photometric techniques, understood as an extension of standard photometric decomposition techniques to the case of IFS data (BUDDI, [14]; C2D, [18]); ii) kinematic decomposition of the spectra into galaxy components [4], and iii) orbital decomposition into dynamically different structures using Schwarzchild modelling [32].

In this work, we explore for the first time the SFR vs. $M_\star$ relation of ETGs separated into their bulge and disc components. To this aim, we use the new algorithm C2D [17] designed to perform spectro-photometric decompositions of galaxy structures using integral field spectroscopy (IFS), in combination with Pipe3D [29], a taylor-made pipeline to retrieve the stellar populations and ionised-gas properties from IFS.

2 The CALIFA sample

A detailed description of the galaxy sample used in this study can be found in [16]. As a brief reminder, we have studied a sample of 129 galaxies drawn from the CALIFA data release 3 (DR3; [28]. The galaxy sample was selected as unbarred following the photometric decomposition analysis of the SDSS imaging presented in [20]. From this work we found that 58 galaxies were well described by a Sérsic bulge and a single exponential disc, 40 galaxies required a broken disc profile in addition to the Sérsic bulge, and 31 are early-type galaxies fitted with a two component model (Sérsic+single exponential) even if their fit is statistically indistinguisable from a single component (pure Sérsic) model (see [19],for details). The spectro-photometric decomposition of our sample into separated bulge and disc datacubes was performed using C2D [18]. The stellar population analysis shown in this paper was performed using the Pipe3D pipeline. This software has been thoroughly applied to

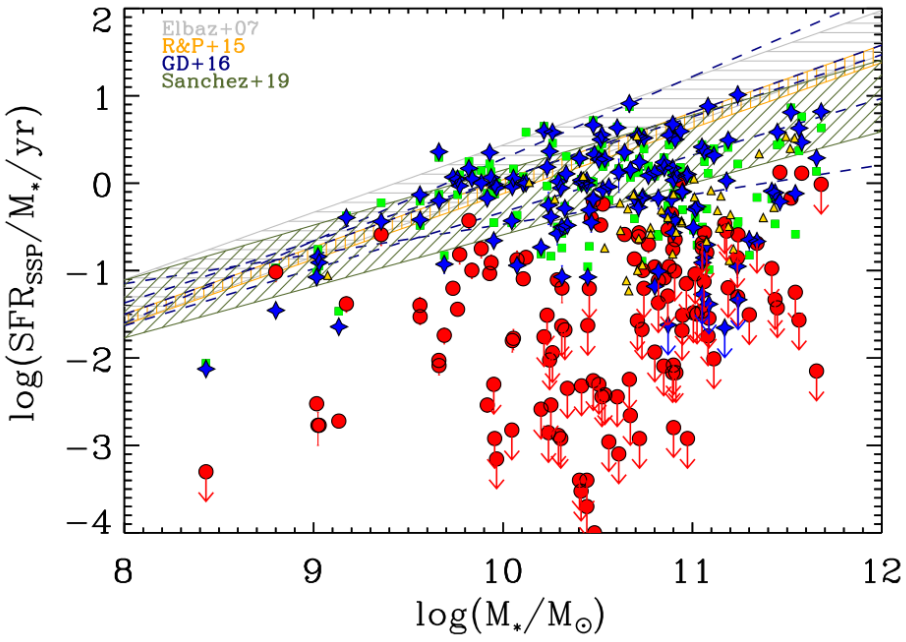

Figure 1: Star formation rate (SFR) vs. galaxy stellar mass. The values for bulges and discs are shown with red circles and blue stars, respectively. Green squares represent measurements of the same galaxies, but considering the galaxy as a whole. Yellow triangles display the control sample of elliptical galaxies. The best fit to the SFMS from Elbaz et al. (2007, Grey), Renzini & Peng (2015, Orange), González Delgado et al. (2016, Navy), Sánchez et al. (2019, Green). Downward arrows mark where the measured SFR is an upper limit (see text for details).

CALIFA data and provides, among others, luminosity/mass weighted ages and metallicities, star formation histories, and intensity maps of strong emission lines for both components [29].

3 The separated SFMS of bulges and discs

Figs. 1 and 2 show the relation between the SFR of our bulges and discs and both the stellar mass of the host galaxy and the stellar mass of each component, respectively. In order to provide a complete picture for our whole sample, we computed the SFR using the analysis of the stellar populations and the recipe given in [13]. We refer the readers to [17] for a detailed description of the process applied to this dataset, and for a discussion on the difference with SFR derived from ionised gas emission lines. The star formation main sequence (SFMS) derived from previous studies in the literature is also shown for comparison, as well as the location of the control sample of ellipticals and the position of the galaxies in the sample if they are considered as a whole.

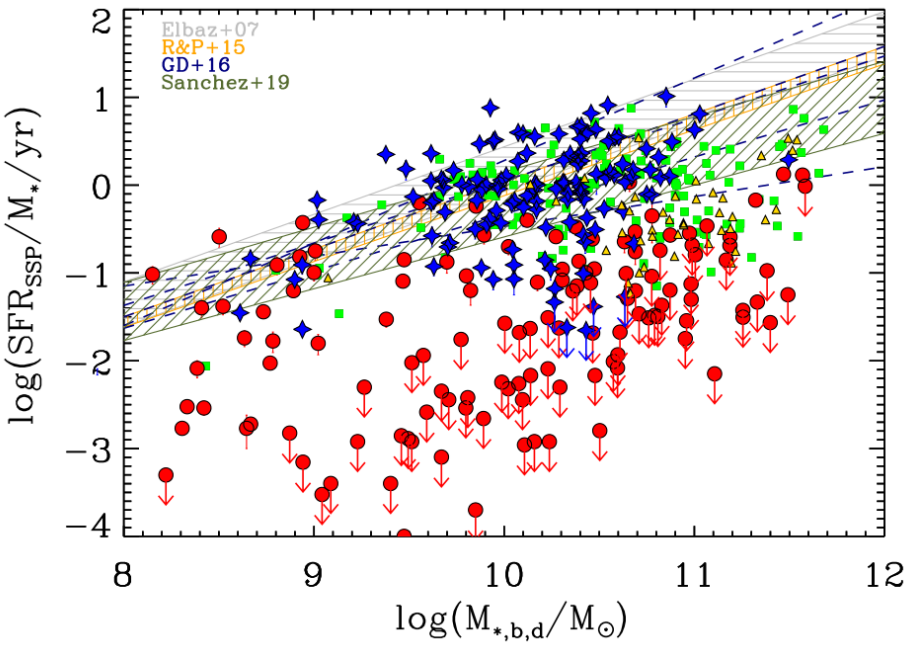

Figure 2: Same as Fig. 1, but using the stellar mass of each component.

The comparison of our bulges and discs with the SFMS derived for star forming galaxies at $z \sim 0$ shows clearly how, independently on which stellar mass is used, most of the discs are compatible with the SFMS whereas most of the bulges lie below this relation, i.e., they are mostly in the region of the diagram occupied by retired galaxies [2]. We find a similar result in [17] using only early type galaxies, and this was also found in [3] for CALIFA galaxies. In particular, we find that, when considering each component stellar mass, 16 (12%) bulges and 99 (77%) discs are compatible (within 1σ) with the SFMS defined in [26]. The fraction of bulges compatible with the SFMS is strongly dependent with the bulge mass. We do not find any bulges compatible with the SFMS in the high mass bin ($\log M_\star/M_\odot > 10.5$), but they reach 38% for bulges with $\log M_\star/M_\odot < 9$. Therefore low-mass bulges are more subject to show recent star formation. The trend is similar for discs even if less dramatic. About 72% of the high-mass discs ($\log M_\star/M_\odot > 10$) lie in the SFMS and this number rises to 91% when considering those with $\log M_\star/M_\odot < 10$. When considering the galaxies as a whole and applying the same analysis, we find that 67% of the galaxies are compatible with the SFMS. Galaxies also show a decline in their fraction of galaxies located in the SFMS with global stellar mass. This is such that 91%, 73%, and 37% of galaxies with masses $9 < \log M_\star/M_\odot < 10$%, $10 < \log M_\star/M_\odot < 11$, and $11 < \log M_\star/M_\odot < 12$ are in the SFMS, respectively. We also computed these fractions as a function of the bulge mass finding that 88%, 59%, and 31% of the galaxies with bulge masses $9 < \log M_\star/M_\odot < 10$, $10 < \log M_\star/M_\odot < 11$, and $11 < \log M_\star/M_\odot < 12$ lie in the SFMS, respectively. Finally, we compare the fraction of bulges and elliptical galaxies that are compatible with the SFMS. We find that, in the mass range where both sample are representative ($10 < \log M_\star/M_\odot < 11.5$), elliptical galaxies are

more prone to star formation (16% in the SFMS) than bulges (3%). Our results are in good agreement with those presented in Lang et al. (2014). Using a separation between star forming galaxies (SFG) and retired galaxies (RG) based on a threshold on their specific SFR (sSFR), they found a strong increase in the fraction of retired galaxies with global galaxy mass and bulge mass, changing from $\sim 10\%$ at $\log M_\star/M_\odot = 10$ to 50% at $\log M_\star/M_\odot = 11.3$. Despite in this work we used the location (or not) of a galaxy with respect to the SFMS to identify SFGs (RGs), the quantitative agreement is remarkable.

Acknowledgments

JMA acknowledges the support of the Viera y Clavijo Senior program funded by ACIISI and ULL. JMA and AdLC acknowledge support from Spanish Ministerio de Ciencia, Innovación y Universidades through grant PID2021-128131NB-I00.

References

[1] Brinchmann, J., Charlot, S., White, S. D. M., et al. 2004, MNRAS, 351, 1151

[2] Cano-Díaz, M., Sánchez, S. F., Zibetti, S., et al. 2016, ApJl, 821, L26

[3] Catalán-Torrecilla, C., Gil de Paz, A., Castillo-Morales, A., et al. 2017, ApJ, 848, 87

[4] Coccato, L., Fabricius, M. H., Saglia, R. P., et al. 2018, MNRAS, 477, 1958

[5] Daddi, E., Dickinson, M., Morrison, G., et al. 2007, ApJ, 670, 156

[6] de Lorenzo-Cáceres, A., Méndez-Abreu, J., Thorne, B., et al. 2020, MNRAS, 494, 1826

[7] de Lorenzo-Cáceres, A., Sánchez-Blázquez, P., Méndez-Abreu, J., et al. 2019b, MNRAS, 484, 5296

[8] de Lorenzo-Cáceres, A., Méndez-Abreu, J., Thorne, B., et al. 2019a, MNRAS, 484, 665

[9] de Lorenzo-Cáceres, A., Falcón-Barroso, J., & Vazdekis, A. 2013, MNRAS, 431, 2397

[10] Ellison, S. L., Teimoorinia, H., Rosario, D. J., et al. 2016, MNRAS, 458, L34

[11] Elbaz, D., Daddi, E., Le Borgne, D., et al. 2007, A&A, 468, 33

[12] González Delgado, R. M., García-Benito, R., Pérez, E., et al. 2015, A&A, 581, A103

[13] González Delgado, R. M., Cid Fernandes, R., Pérez, E., et al. 2016, A&A, 590, A44

[14] Johnston, E. J., Häußler, B., Aragón-Salamanca, A., et al. 2017, MNRAS, 465, 2317

[15] Lang, P., Wuyts, S., Somerville, R. S., et al. 2014, ApJ, 788, 11

[16] Méndez-Abreu, J., de Lorenzo-Cáceres, A., & Sánchez, S. F. 2021, MNRAS, 504, 3058

[17] Méndez-Abreu, J., Sánchez, S. F., & de Lorenzo-Cáceres, A. 2019b, MNRAS, 488, L80

[18] Méndez-Abreu, J., Sánchez, S. F., & de Lorenzo-Cáceres, A. 2019a, MNRAS, 484, 4298

[19] Méndez-Abreu, J., Aguerri, J. A. L., Falcón-Barroso, J., et al. 2018, MNRAS, 474, 1307

[20] Méndez-Abreu, J., Ruiz-Lara, T., Sánchez-Menguiano, L., et al. 2017, A&A,a 598, A32

[21] Méndez-Abreu, J., Debattista, V. P., Corsini, E. M., et al. 2014, A&A, 572, A25

[22] Méndez-Abreu, J., Aguerri, J. A. L., Corsini, E. M., et al. 2008, A&A, 478, 353

[23] Noeske, K. G., Weiner, B. J., Faber, S. M., et al. 2007, ApJl, 660, L43

[24] Renzini, A. & Peng, Y. 2015, ApJl, 801, L29

[25] Saintonge, A., Tacconi, L. J., Fabello, S., et al. 2012, ApJ, 758, 73

[26] Sánchez, S. F., Avila-Reese, V., Rodríguez-Puebla, A., et al. 2019, MNRAS, 482, 1557

[27] Sánchez, S. F., Avila-Reese, V., Hernandez-Toledo, H., et al. 2018, RMA&A, 54, 217

[28] Sánchez, S. F., García-Benito, R., Zibetti, S., et al. 2016, A&A, 594, A36

[29] Sánchez, S. F., Pérez, E., Sánchez-Blázquez, P., et al. 2016, RMA&A, 52, 21

[30] Willett, K. W., Schawinski, K., Simmons, B. D., et al. 2015, MNRAS, 449, 820

[31] Wuyts, S., Förster Schreiber, N. M., van der Wel, A., et al. 2011, ApJ, 742, 96

[32] Zhu, L., van de Ven, G., Leaman, R., et al. 2020, MNRAS, 496, 1579